Small-x behavior of the singlet polarized structure function g_2 in the double logarithmic approximation

J. Bartels
II.Institut f. Theoretische Physik, Universität Hamburg, D-20355 Hamburg, Germany

M. G. Ryskin
Petersburg Nuclear Physics Institute, Gatchina, S.-Petersburg 188300, Russia

(Received 20 February 2002; published 20 June 2002)

The small-x behavior of the singlet contributions to the polarized structure function $g_2(x,Q^2)$ is calculated in the double-logarithmic approximation of perturbative QCD. The dominant contribution is due to the gluons which, in contrast with the unpolarized case, mix with the fermions also in the small-x domain. We find a powerlike growth in $1/x$ in the odd-signature parts of the amplitude with the same power as in the singlet function $g_1(x,Q^2)$ at $x \ll 1$.

DOI: 10.1103/PhysRevD.65.114012 PACS number(s): 12.38.Bx, 13.60.Hb, 14.20.Dh

I. INTRODUCTION

The investigation of the structure functions g_1 and g_2 provides the basis for the theoretical description of polarization effects in deep inelastic lepton nucleon scattering. The Q^2 evolution of the spin dependent function g_1 is well known: at $x \sim 0(1)$ one can use the original Altarelli-Parisi equations [1], whereas in the region of very small x the double logarithmic approximation [2,3] has to be used and predicts a stronger growth in $1/x$ than the Altarelli-Parisi equations. The situation with the other polarized structure function g_2 is more complicated. Compared to g_1, several new features appear [4].

First, there exists a twist-3 contribution to g_2, $g_2^{(3)}$, which is not suppressed even for large Q^2 [5]. Part of the function g_2 may be obtained from the known structure function $g_1(x,Q^2)$ with the help of the Wandzura-Wilczek relation [6], and from another integral relation [7] which relates the twist-3 piece of g_2 to the (m^2/Q^2 suppressed) twist-3 corrections to g_1. However these relations are not enough to restore the whole spin dependent function $g_2(x,Q^2)$. This can be seen from the explicit one loop calculation of $g_2(x,Q^2)$ on a quark target [8,9][1] and also from the small-x behavior of the nonsinglet component of $g_2(x,Q^2)$, calculated in the double logarithmic approximation (DLA) in [4].

Another distinct feature and difference from the standard leading-twist evolution equations is the fact that the number of operators which contribute to the twist-3 component of $g_2(x,Q^2)$, $g_2^{(3)}$, is not fixed but increases with the moment index n (see, e.g. [11,12]). Nevertheless, in the two limits, (i) $n \to \infty$ [where n denote the (x) moments] and (ii) number of colors $N_c \to \infty$, it has been shown that the quark-gluon operators decouple from the quark operator evolution equation [13], and the asymptotic behavior of $g_2(x,Q^2)$ in the region $1-x \ll 1$ has been derived.[2]

Next, in the region of small x g_2 has to be decomposed into pieces with different signatures. Whereas unpolarized structure functions and the polarized structure function g_1 have a definite signature (e.g., g_1 is the energy discontinuity of an odd-signature scattering amplitude), g_2 contains both even and odd signature [17,18], and an important part of the small-x analysis of g_2 is the separation of the two signature structures. Because of the different contents of signature, g_1 and g_2 are expected to have a different behavior near $x=0$ (i.e. different powers of $1/x$; see, for example, [17,19]).

Finally, in the region of small x another new feature arises. It is well known that the strong ordering of transverse momenta is violated [2,19–21]. Instead of $k_{i,t}^2 \gg k_{i-1,t}^2$ one has $k_{i,t}^2 \gg (x_i/x_{i-1}) k_{i-1,t}^2$ (with $x_i \ll x_{i-1}$). As a result, double log contributions of the form $(\alpha_s \ln^2 1/x)^n$ appear which cannot be summed up in the framework of the conventional $\log Q^2$ evolution. This feature holds for both g_1 and g_2, and for g_1 it has been discussed in detail in [2,3]. In particular, the infrared evolution equation (IREE) [19] has been used to sum up all the leading perturbative QCD (PQCD) double logarithms (DL) of the form $\alpha_s^n \ln^k 1/x \ln^m Q^2$ with $m \leqslant n$ and $k+m=2n-1$. In [4] similar techniques have been used to investigate the small-x behavior of the polarized structure function g_2: so far only the nonsinglet case has been analyzed. In this paper we present the study of the singlet part of g_2, and we find its asymptotic behavior at $x \to 0$. In analogy with our study of the nonsinglet part of g_2 we consider the scattering amplitude of a virtual photon and a quark. We will not (yet) address the question of how our calculations can be used for the polarized structure function g_2 of the proton, i.e. how to set up the initial conditions coming from the confinement region.

[1] The one loop function $g_2(x,Q^2)$ on the gluon target was calculated in [10].

[2] See also [14] for a recent study of the twist-3 ($g_2^{(3)}$) evolution in the $N_c \to \infty$ limit, [15] for the QCD evolution of twist three operators beyond the large-N_c limit, and [16] for a possibility to study the scale dependence of $g_2(x,Q^2)$ beyond the $N_c \to \infty$ limit.

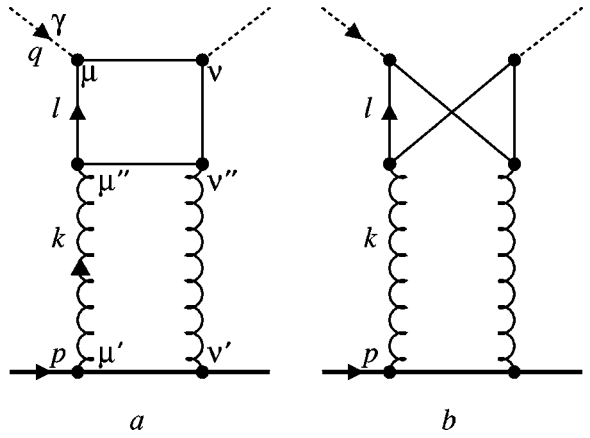

FIG. 1. The lowest order Feynman diagrams which contain a gluon *t*-channel state.

In [4] we have shown that, for the even signature part of the nonsinglet g_2, the only double logarithmic contributions come from the ladder-type Feynman diagrams with *t*-channel intermediate states consisting of two quarks only. For the odd-signature part of the amplitude one has to consider also nonladder graphs where an additional ''soft'' *t*-channel gluon ''embraces'' a part of the ladder diagram, in which the transverse momenta of all partons (gluons and quarks) are larger than the transverse momentum of this ''embracing'' soft gluon. The DL contribution of such a graph can be summed up by the IREE, using the method proposed in [19]. In [4] we have analyzed all one and two loop diagrams, contributing to the nonsinglet component of g_2, and we extracted the double logarithms. In the singlet part of g_2, whose analysis is the goal of the present paper, there are only two new 2-loop diagrams, shown in Fig. 1. Figure 1(a) has the same ladder structure but with the two-gluon *t*-channel intermediate state while the crossed box diagram of Fig. 1(b), as usual, loses the logarithm. The analysis of these graphs, together with the results of [4], will enable us to find the small-x behavior of the singlet g_2 structure function.

A comment is in order about the contribution of *t*-channel states with more than two gluons. For unpolarized structure functions at very small x, diagrams with any number of *t*-channel gluons contribute to the small-x behavior of the scattering amplitude $\sim 1/x$ (modulo powers of $\ln 1/x$). For the polarized case (both g_1 and g_2) the antisymmetric tensor structure (see below) requires, for the two gluon state, the polarization of the *t*-channel gluons to be different from each other; as a result, the amplitude behaves as $\sim x^0$ (modulo powers of $\ln 1/x$). Consequently, even at small x, quark and gluon *t*-channel states mix, quite in contrast to the unpolarized case. However, also in the polarized case, there exist *t*-channel states of gluons which lead to a small-x behavior $\sim 1/x$. The simplest one [22] consists of three gluons, has positive C parity, and is dual to the odderon solution discussed in [23]. This three gluon contribution, however, is beyond the DL approximation used in this paper. First, the coupling of this state to the virtual photon is suppressed by a few extra powers of α_s which are not accompanied by the maximal number of logarithms. Next, the contribution of this state to g_2 is suppressed by an extra power of $1/Q^2$, needed to compensate the dimension of the transverse momenta k_{1t}, k_{2t} (of the gluons) which saturate the antisymmetric tensor $\varepsilon^{\mu\nu\alpha\beta}$, and reflecting the orbital momentum in the three gluon state. For these reasons, contributions from diagrams with more than two gluons will not be considered in this paper.

The outline of the paper is as follows. In Sec. II we consider the kinematics of the process and outline our strategy. In Sec. III we calculate the DL small-x contribution of the simplest singlet diagrams shown in Fig. 1. It turns out that the DL asymptotics of Fig. 1 is proportional to the singlet structure function $g_1(x,Q^2)$. Based on this general property we consider in Secs. III and IV the small-x behavior of the spin dependent function $g_2(x,Q^2)$. Sections V and VI contain the evolution equations and their solutions. In a concluding section we present a brief summary.

II. KINEMATICS AND DEFINITIONS

Let us begin with a brief summary of previous results and with an outline of our future strategy. The spin dependent part of the hadronic tensor $iW^A_{\mu\nu}$ of the deep inelastic scattering (DIS) lepton-quark scattering amplitude has the form

$$T^A_{\mu\nu}=\frac{M}{(pq)}i\varepsilon^{\mu\nu\alpha\beta}\Big[q_\alpha s_\beta T_1(x,Q^2) + q_\alpha\Big(s_\beta-\frac{(sq)}{(pq)}p_\beta\Big)T_2(x,Q^2)\Big], \tag{1}$$

where M,p_μ and s_μ denote the mass, the four momentum and the spin (pseudo)vector of the target, respectively. As usual, $(sp)=0$ and $s^2=-1$, and the spin-dependent structure functions are defined as the discontinuities of T_1 and T_2:

$$g_{1,2}=-\frac{1}{2\pi}\mathrm{Im}\,T_{1,2}. \tag{2}$$

Throughout this paper we work in the Feynman gauge and use the Sudakov representation of the momenta of quarks and gluons:

$$k_i=-\alpha_i q'+\beta_i p+k_{ti}. \tag{3}$$

The photon four momentum is written as $q=q'-xp$, and p and q' are the two lightlike reference vectors. The Jacobian can be written as

$$d^4k_i=\frac{S}{2}d\alpha_i d\beta_i d^2k_{ti}. \tag{4}$$

Here $S=2q'p$ denotes the center of mass energy, and we assume that the quark target mass is small: $M^2\ll Q^2=-q^2$. So one may neglect the value of this mass M everywhere, except for the mass term in the target density matrix. This mass term is needed in order to obtain a nonzero spin trace

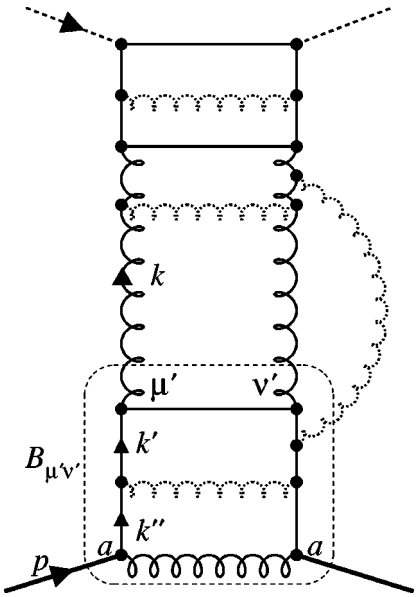

FIG. 2. A generic Feynman diagram for the scattering of a virtual photon on a quark target.

proportional to the first power of M [see Eq. (1)].[3] Finally, we recall from [4] that, in order to obtain in Eq. (1) a nonzero contribution to g_2, we need a transverse polarization of the target ($s_\mu = s_{\mu t}$): longitudinal polarization of the target $s_\mu = p'_\mu/m$ contributes to the structure function g_1 only, while the transverse ($s_\mu = s_{t\mu}$) polarization gives the sum $g_\perp = g_1 + g_2$.

Let us briefly recapitulate our previous analysis of the polarized structure function. Consider a generic ladder diagram (Fig. 2) and begin at the bottom. Since the spin dependent part of the hadronic tensor $W_{\mu\nu}$ is antisymmetric (proportional to the ε tensor), in the target density matrix we have to start from the $\gamma_5 \hat{s}$ part:

$$\frac{1}{2}(\hat{p}+m)(1-\gamma_5\hat{s}). \tag{5}$$

When calculating the trace, this γ_5 matrix gives the antisymmetric tensor $\varepsilon^{\mu\nu\alpha\beta}$. As we have said before, for the present analysis we chose transverse polarization of the target quark.

Moving upwards inside the ladder diagrams, we encounter t-channel intermediate states which consist of a quark-antiquark pair of two gluons. For the quark t-channel state, we have found in [4] two different polarization structures which we will denote by $'s'$ and $'k'$:

$$'s' \Rightarrow \gamma_5 \hat{s}_t, \tag{6}$$

$$'k' \Rightarrow (2sk)\cdot\gamma_5\hat{k}, \tag{7}$$

where k_μ is the t-channel quark momentum. At the target we begin with the "s" structure, but at any gluon rung above we have both possibilities: either to continue with "s" or start a "k branch." The latter continues with "k" structures only, until at the upper end of the diagram it ends with the coupling to the photon. There is no return from a "k branch" to an "s branch." Moreover, the "k branch" contains only odd signature, and its evolution is the same as in g_1, whereas the "s branch" contains both even and odd signature and has slightly modified evolution equations. Nonladder structures cancel for even signature branches, whereas for odd signature they lead to an additional term in the evolution equation.

What is new in the present singlet case is the two-gluon intermediate state. We first note that this intermediate state must have the same antisymmetric structure (with respect to the gluon polarizations μ' and ν') as the ε polarization tensor. Thus we cannot assign to both gluons the same longitudinal polarizations which would lead to the small-x behavior $\sim 1/x$. The best one can do for retaining the largest power of $1/x$ is to assign the longitudinal polarization ($e_{\mu'} \propto q'_{\mu'}$) to one of the two gluons and the transverse polarization ($e_{\nu'} = e_{\nu' t}$) to the other gluon. Therefore, as mentioned before, in contrast to the unpolarized structure function $f_1(x,Q^2) \sim 1/x$, the prediction for the small-x behavior of the polarized distributions goes as

$$g_{1,2}(x,Q^2) \sim \text{const} \times F(\alpha_s \ln Q^2 \ln 1/x, \alpha_s \ln^2 1/x), \tag{8}$$

where the function F denotes the leading (DL) corrections to the asymptotics of the Born singlet spin dependent structure function: $g_{1,2}(x,Q^2) \sim \text{const}$ as $x \to 0$. Speaking in terms of the complex angular momentum j plane, both the two t-channel quark and two gluon exchange lead to the rightmost singularity at $j = \omega = 0$, and even at very small x for the singlet spin dependent structure functions we have to account for the transitions between the quark and gluon t channel states. Continuing with the spin structure of the t-channel two gluon state we have to recall that the longitudinal gluon polarization $e_{\mu'}$ is contained in the term $q'_{\mu'} p'_{\mu''}/(q'p')$ in the spin part of the gluon propagator

$$d_{\mu'\mu''} = g_{\mu'\mu''} = g^{\perp}_{\mu'\mu''} + \frac{p'_{\mu'} q'_{\mu''} + q'_{\mu'} p'_{\mu''}}{(p'q')}, \tag{9}$$

where the vector $q'_{\mu'}$ ($p'_{\mu''}$) is contracted with the spin structure at the lower (upper) end of the t-channel gluon. The transverse polarization is contained in $g^{\perp}_{\mu'\mu''}$. At first sight there are two antisymmetric spin structures with one longitudinal gluon:

$$\text{(a)} \qquad \varepsilon^{\mu\nu\alpha\beta} s^{\perp}_{\alpha} p'_{\beta} \tag{10}$$

and

$$\text{(b)} \qquad s^{\perp}_{\mu} p'_{\nu} - p'_{\mu} s^{\perp}_{\nu}\,.$$

However, the last structure has unnatural parity (s_μ is a pseudovector) and never contributes to our amplitude Eq. (1). So it is enough to consider the first structure, Eq. (10), only. Since this structure is the same as in the case of g_1, we can make use of the results of [3].

[3]Hence we may put $p^2 \simeq p'^2 = 0$.

It will be the central task of this paper to compute the evolution kernels of the different t-channel states and the transitions from one to another. Altogether, we have three different states: the two spin structures of quark-antiquark states, Eqs. (6) and (7), and the two gluon state. As usual, the DL contribution comes from the kinematical region of

$$1 \gg \beta_1 \gg \beta_2 \gg \cdots > x$$

and

$$\cdots \ll \alpha_1 \ll \alpha_2 \ll \cdots \ll 1. \tag{11}$$

The contour of the α_i loop integration will be closed around the pole of the propagator of the i-th s-channel (horizontal line) particle. Thus all the s-channel particles lie on mass shell, and the t-channel propagators can be approximated by $1/k_i^2 \simeq /k_{it}^2$, as $\alpha_i \beta_i s \ll k_{it}^2$. So the i-th loop integral takes the form

$$C \frac{\alpha_s}{2\pi} \frac{d\beta_i}{\beta_i} \frac{dk_{it}^2}{k_{it}^4} \times \text{numerator}. \tag{12}$$

The logarithmic β_i integration is written explicitly, while, in order to obtain the second logarithm (from the integral over dk_{it}^2), we need to select the term proportional to k_{it}^2 in the numerator, coming from the spin part of the diagram. As discussed before, the gluon→gluon case we take from [3]; the evolution of the ''s branch'' and ''k branch'' quark structures were obtained in [4], the transition from ''s branch'' to ''k branch'' is also contained in [4], and the transition from '' k branch'' to ''s branch'' vanishes. Collecting these results in terms of a matrix whose columns (rows) are labeled by the spins structure of the t-channel states below (above) the transition, we have for the numerator in Eq. (12)

$$\begin{pmatrix} gg & kg & sg \\ gk & kk & sk \\ gs & ks & ss \end{pmatrix} = \begin{pmatrix} 4 & -1 & ? \\ 2 & 1 & 0 \\ ? & -1 & 1 \end{pmatrix}. \tag{13}$$

Here the labels (g, k, s) refer to the spin structures of the gluon, the ''k'' structure of the quark and the ''s'' structure of the quark, respectively The 2×2 block matrix in the upper left corner coincides with g_1^s and has been taken from [3]; the 2×2 block matrix in the lower left corner, on the other hand, is the same as in the nonsinglet g_2 case and has been derived in [4]. What still needs to be computed are the matrix elements denoted by ''?'': in the two following sections we will show that both elements vanish.

The color factors C are the same as in the unpolarized scattering: for the gluon→gluon it is equal to $C_A = N_c$ ($N_c = 3$ is the number of colors), for the quark → gluon and quark → quark splitting we have $C_F = (N_c^2 - 1)/2N_c$, and for the gluon → quark transition the color factor is $2T_F = n_F$ (n_F is the number of light quark flavors). Combining these color factors with the elements of the numerators matrix in Eq. (13), we have all ingredients to the infrared evolution equations.

III. SINGLET TWO-LOOP DIAGRAM

We start with the amplitude Fig. 1(a) and use the transverse vector $s_{t\mu}$ The spin dependent lower part of Fig. 1(a) takes the form

$$B_{\mu'\nu'} = -\frac{1}{2}\mathrm{Tr}[\gamma_{\nu'}(\hat{p}+m)\gamma_5 \hat{s}\gamma_{\mu'}(\hat{p}-\hat{k}+m)]$$
$$= -2i\varepsilon^{\mu'\nu'\alpha\beta} s_\alpha^\perp k_\beta, \tag{14}$$

where in order to obtain the leading (in $1/x$) contribution we have to keep the longitudinal component of the gluon momentum $k_\beta \simeq \beta p'_\beta$.

Next, to simplify the calculation of the trace of the upper quark loop we make use of gauge invariance. The amplitude $U^{\mu\nu}_{\mu''\nu''}$, which corresponds to the upper block and includes both the box [Fig. 1(a)] and crossed box [Fig. 1(b)] diagrams, satisfies the properties

$$U^{\mu\nu}_{\mu''\nu''} \cdot q_\mu = 0 \tag{15}$$

and

$$U^{\mu\nu}_{\mu''\nu''} k_{\mu''} = U^{\mu\nu}_{\mu''\nu''}(k_t + \beta p' - \alpha q')_{\mu''} = 0. \tag{16}$$

Based on the gluon gauge invariance (16) one may replace the momentum $p'_{\mu''}$ in the longitudinal gluon polarization vector [i.e. the spin part of the gluon propagator (9)] by $-k_{t\mu''}/\beta$; the contribution of the term $-\alpha q'_{\mu''}$ does not contain the double logarithm and may be neglected within the kinematical domain (11). We contract the tensor in Eq. (14) with the gluon numerators (9) and make use of this replacement. The polarization of the t-channel gluons is then described by the tensor structure

$$T_{\mu''\nu''} \propto \frac{\tilde{e}_{\mu''} k_{t\nu''} - k_{t\mu''} \tilde{e}_{\nu''}}{\beta}$$
$$= \frac{(ks^\perp)}{\beta} \varepsilon^\perp_{\mu''\nu''}$$
$$= \frac{(ks^\perp)}{(p'q')\beta} \varepsilon_{\mu''\nu''\alpha\beta} p'_\alpha q'_\beta,$$

where $\varepsilon^\perp_{\mu\nu}$ is the two dimensional antisymmetric tensor, and the polarization vector has the form $\tilde{e}_{\mu''} = \varepsilon^\perp_{\mu''\alpha} s^\perp_\alpha$. In this way the expression (14) can be rewritten as

$$B_{\mu''\nu''} \simeq 2i\beta\varepsilon^{\mu''\nu''\alpha\beta} p'_\alpha s^\perp_\beta \Rightarrow 2i \frac{(ks^\perp)}{(p'q')} \varepsilon^{\mu''\nu''\alpha\beta} p'_\alpha q'_\beta. \tag{17}$$

Since the transverse spin vector $s_{t\mu}$ corresponds to the spin-flip amplitude from the photon side we choose one transverse and one longitudinal photon polarization vector, $E_\mu = E^\perp_\mu$ and $E_\nu = E^\parallel_\nu = (1/\sqrt{Q^2})(q' + xp')$. With the help of the photon

gauge invariance (15) the last vector can be replaced by $E^{\parallel}_{\nu}=2xp'/\sqrt{Q^2}$. Thus, finally, in the case of Fig. 1(a) we have to calculate the trace

$$\mathrm{Tr}^a=\frac{2i(ks^{\perp})}{(p'q')}\varepsilon^{\mu''\nu''\alpha\beta}p'_{\alpha}q'_{\beta} \times[\gamma''_{\nu}\hat{l}\hat{E}^{\parallel}(\hat{q}+\hat{l})\hat{E}^{\perp}\hat{l}\gamma''_{\mu}(\hat{l}-\hat{k})]. \tag{18}$$

Using the identity

$$\gamma_{\nu}\hat{k}\gamma_{\mu}=-i\varepsilon_{\mu\nu\lambda\sigma}k_{\lambda}\gamma_5\gamma_{\sigma} +(\text{the term symmetric under } \mu\rightleftharpoons\nu) \tag{19}$$

we obtain

$$\mathrm{Tr}^a=\frac{4(ks^{\perp})}{(p'q')}\{(p'(l-k))\mathrm{Tr}[\gamma_5\hat{q}'\hat{l}\hat{E}^{\parallel}(\hat{q}+\hat{l})\hat{E}^{\perp}\hat{l}] -(q'(l-k))\mathrm{Tr}[\gamma_5\hat{p}'\hat{l}\hat{E}^{\parallel}(\hat{q}+\hat{l})\hat{E}^{\perp}\hat{l}]\}. \tag{20}$$

Putting in Eq. (20) $E^{\parallel}=2xp'/\sqrt{Q^2}$, it is easy to see that the largest (and the only DL) contribution (where q' is multiplied by the momentum k, and p' by momentum l'; note that $\alpha_l\gg\alpha_k$ and $\beta_k\gg\beta_l$) comes from the second term and reads

$$\mathrm{Tr}^a\approx\frac{4(ks^{\perp})}{(p'q')}(q'k)(2p'l)\mathrm{Tr}[\gamma_5\hat{E}^{\parallel}\hat{q}\hat{E}^{\perp}\hat{l}]. \tag{21}$$

As the s-channel quark with momentum $(k-l)$ is on mass shell, the product $(q'k)(2p'l)/(q'p')=-\beta_k\alpha_l s\simeq(k-l)_t^2$. So after the azimuthal angular integration we get

$$4(ks^{\perp})(k-l)_t^2l_{\mu}=2k_t^2l_t^2s^{\perp}_{\mu},$$

that is

$$\mathrm{Tr}^a\simeq 2k_t^2l_t^2\mathrm{Tr}[\gamma_5\hat{E}^{\perp}\hat{E}^{\parallel}\hat{q}\hat{s}^{\perp}]\Rightarrow i\varepsilon^{\mu\nu\alpha\beta}q_{\alpha}s^{\perp}_{\beta}(8k_t^2l_t^2), \tag{22}$$

where the first factor is exactly the structure we are looking for in the hadronic tensor (1), and the last factor $8k_t^2l_t^2$ is needed to keep the leading logarithms in the dk_t^2 and dl_t^2 integrations, as was discussed at the end of Sec. II.

Finally, let us consider the trace corresponding to the crossed box diagram of Fig. 1(b):

$$\mathrm{Tr}^b=2i\frac{(ks^{\perp})}{(p'q')}\varepsilon^{\mu\nu\alpha\beta}p'_{\alpha}q'_{\beta}\mathrm{Tr}[\gamma_{\nu}(\hat{q}+\hat{l}-\hat{k}) \times\hat{E}^{\parallel}(\hat{l}-\hat{k})\gamma_{\mu}\hat{l}\hat{E}^{\perp}(\hat{q}+\hat{l})]. \tag{23}$$

The product of the three γ-matrices $[\hat{l}\hat{E}^{\perp}(\hat{q}+\hat{l})]$ may be decomposed as

$$\hat{l}\hat{E}^{\perp}(\hat{q}+\hat{l})=c_{\delta}\gamma_{\delta}+d_{\delta}\gamma_5\gamma_{\delta}. \tag{24}$$

The last term has unnatural parity and may be neglected, while the vector $c_{\delta}=\frac{1}{4}\mathrm{Tr}[\hat{l}\hat{E}^{\perp}(\hat{q}+\hat{l})\gamma_{\delta}]$. Using this fact and the identity (19) we get

$$\mathrm{Tr}^b=\frac{(ks^{\perp})}{(p'q')}\{\mathrm{Tr}[\hat{p}'\hat{l}\hat{E}^{\perp}(\hat{q}+\hat{l})] \times\mathrm{Tr}[\gamma_5\hat{q}'(\hat{q}+\hat{l}-\hat{k})\hat{E}^{\parallel}(\hat{l}-\hat{k})]-\mathrm{Tr}[\hat{q}'\hat{l}\hat{E}^{\perp}(\hat{q}+\hat{l})] \times\mathrm{Tr}[\gamma_5\hat{p}'(\hat{q}+\hat{l}-\hat{k})\hat{E}^{\parallel}(\hat{l}-\hat{k})]\}. \tag{25}$$

The second trace in the first term on the right-hand side (RHS) of Eq. (25) vanishes as it contains only one transverse vector $(l-k)_t$, while the last term in Eq. (25) is zero since in the second trace $E^{\parallel}_{\mu}\propto p'_{\mu}$. Therefore we neglect the crossed box contribution (after the trick based on the gauge invariance was applied) and the whole DL result, given by the ladder-type Fig. 1 diagrams, reads

$$g_{\perp}^s(x)=-e_q^2\cdot 2c_F\left(\frac{\alpha_s}{2\pi}\right)^2\int\frac{d\beta_k}{\beta_k}\int\frac{dk_t^2}{k_t^2}\int\frac{dl_t^2}{l_t^2} \tag{26}$$

(here e_q is the electric charge of the quark). In Eq. (26), the limits of integration follow from Eq. (11) and the discussion after Eq. (11).

We have to note that, within the DL approximation, the result (26) for $g_{\perp}=g_1+g_2$ coincides with the lowest order singlet function g_1^s. In other words, to this order of accuracy we obtain the singlet $g_2^s(x)=0$. This is the consequence of the fact that in the lower part of the Fig. 1 graph the Born structure function $g_2^B=0$. For the one loop approximation (order α_s) it is known [8] that at small x the one loop result is given by

$$g_2(x,Q^2)\simeq\frac{e_q^2C_F\alpha_s}{2\pi}x\ln\frac{Q^2}{m^2x},$$

i.e. is much smaller than

$$g_1(x,Q^2)\sim\frac{e_q^2C_F\alpha_s}{2\pi}\ln\frac{Q^2}{m^2x}.$$

So it is only at the two loop level (or above) that the nonsinglet structure function $g_2^{n.s.}$ becomes comparable to the value of $g_1^{n.s.}$ at $x\ll 1$. Thus one expects a nonzero DL contribution to the small-x behavior of the singlet g_2 component at earliest at two loops. Our result (26), however, shows that at the two loop level it still vanishes. We therefore have to turn to three or more loops. On the other hand, we know already from the argument given in Sec. II that in the DL approximation the gluon contributions both to $g_{\perp}=g_1+g_2$ and to g_1 are driven by the same spin structure (10). Therefore we may expect that the distributions g_2^s and g_1^s will have the same asymptotic small-x behavior. In the following section we will show that this is indeed the case.

IV. HIGHER ORDER CONTRIBUTIONS

We now turn to higher order corrections to Figs. 1(a) and 1(b). As a generic diagram, we consider Fig. 2. Beginning with the quark target at the bottom, we first have the same evolution as in the nonsinglet case. After the first *s*-channel gluon the initial quark density matrix $\frac{1}{2}(\hat{p}+m)(1-\gamma_5\hat{s})$ gives

$$\frac{1}{2}\sum_a \gamma_a(\hat{p}+m)(-\gamma_5\hat{s})\gamma_a = m\gamma_5\hat{s}, \tag{27}$$

where we omit the terms which do not depend on the quark spin vector s_μ. In this way we obtain the structure $\gamma_5\hat{s}$. At the next step this spin structure, together with the *t*-channel quark propagators $\hat{k}''$, produces the second structure $(2sk)\cdot\gamma_5\hat{k}$:

$$\hat{k}''\gamma_5\hat{s}\hat{k}'' = (k''^2)\gamma_5\hat{s} - (2sk'')\cdot\gamma_5\hat{k}''. \tag{28}$$

Consequently, starting from two *s*-channel gluons, the quark density matrix in the upper (k') cell of the block contains the two structures $\gamma_5\hat{s}$ and $(2s^\perp k')\gamma_5\hat{k}'$. So our diagram splits into two branches, and we have to follow each branch separately. The latter one, $\gamma_5\hat{k}'$, is equivalent to the density matrix of a longitudinally polarized quark with the momentum k'_μ. So this spin dependent part of the heavy photon-quark k' amplitude is described by the photon-quark structure function $g_1(\gamma^*q)$

$$T_{\mu\nu}(\gamma^*q) = \frac{i\varepsilon^{\mu\nu\alpha\beta}}{(k'q)}q_\alpha\cdot k'_\beta\cdot T'_1(x',Q^2) \tag{29}$$

with $\mathrm{Im}\,T'_1 = -2\pi g_1(\gamma^*q)$ and $x' = Q^2/2(k'q)$. The integration over the azimuthal direction of the vector k'_t $(\int d\varphi(2s^\perp k^\perp)k'_\mu = k_t^2 s^\perp_\mu)$ replaces the tensor $\varepsilon^{\mu\nu\alpha\beta}q_\alpha k'_\beta$ by $\varepsilon^{\mu\nu\alpha\beta}q_\alpha s^\perp_\beta$ and gives the factor $k_t'^2$ needed to save the DL structure of the $dk_t'^2$ integral. As a result, the branch in $g_\perp$ which originates from the "*k*" quark structure, $2(s^\perp k')\gamma_5\hat{k}'$, is proportional to g_1^s. So we can make use of our results [3] for g_1^s: we know the transitions from the gluon *t*-channel to the quark *t*-channel (and vice versa), and we also know the latter never contains the "*s*" spin structure. In other words, we have shown that in Eq. (13) the upper right element, sg, vanishes.

Following the other branch, which starts from the "*s*" structure, $\gamma_5\hat{s}^\perp$, at the upper end of the lower block, we note that it does not lead to any double logarithm at all. To show this we again make use of the gauge invariance, that is the condition analogous to Eq. (16) but with respect to the lower block: $B_{\mu'\nu'}k_{\mu'}=0$. Based on this condition we replace the vector q' by $-k_{t\mu'}/\alpha_k$. After this, the polarization of the only *t*-channel gluon state which may give the DL's is described by the pure transverse tensor $T_{\mu'\nu'}\propto\varepsilon^\perp_{\mu'\nu'}\cdot(ks^\perp)/\alpha$. On the other hand, the $\gamma_5\hat{s}^\perp$ quark structure produces the tensor $B_{\mu'\nu'} = -4i\varepsilon^{\mu'\nu'\alpha\beta}s^\perp_\alpha(k'-k)_\beta$ orthogonal to $\varepsilon^\perp_{\mu'\nu'}$. As a result, in DL we have no transition from the "*s*" structure to gluon states: in the lower left element, gs vanishes.

In summary, the DL singlet contributions start from the $\gamma_5\hat{k}'$ quark structure, and the gluon evolution is the same as in g_1^s. It therefore may be written as the convolution of the nonsinglet structure function g_2 with the singlet function g_1^s. Note that we have to use not the whole DL nonsinglet function $g_2^{n.s.}$, but only its part g_2^k which corresponds to the structure $\gamma_5\hat{k}'$. This part can be easily extracted from Ref. [4], while the DL singlet function g_1^s needed in the convolution can be taken from [3].

This value of ω_s is considerably larger than the value of corresponding "intercept" of the nonsinglet function $g_2^{n.s.}$, where $\omega_{n.s.}=\omega_0=\sqrt{(2C_F\alpha_s)/\pi}$ (the ratio of the two values ω_s/ω_0 is about 2.6). Therefore the asymptotic behavior of the spin dependent singlet structure function $g_2^s(x,Q^2)$ is almost completely driven by the DL behavior of the singlet $g_1^s(x,Q^2)$ distribution.

Let us return to the signature question. As we have mentioned in Sec. II, the analysis of the nonsinglet case in [4] has shown that the "*s*" branch of the quark state contains contributions to both signatures, whereas the "*k*' branch has negative signature only. Since in our DL approximation the two gluon state communicates only with the "*k*" branch, it connects to negative signature only. The only place where even signature can appear is the "*s*" structure of the quark state which is the same as in the nonsinglet function $g_2^{n.s.}$.

The negative signature in the gluon *t*-channel state can be seen rather directly. Indeed, as it was discussed in [4], one obtains the negative signature term keeping the photon (or gluon) momentum in the trace over the quark loop. In the quark→gluon transition the trace reads

$$\mathrm{Tr}^{gq} = \mathrm{Tr}[\gamma_5\hat{k}'\gamma_{\nu'}(\hat{k}'-\hat{k})\gamma_{\mu'}], \tag{30}$$

where the gluon momentum *k* gives the only nonzero contribution. The same can be seen in the gluon to quark transition. Recall our two loop calculation of Sec.III. Here the leading DL contributions come from the second term on the right-hand side (RHS) of Eq. (20). In this term we have to keep the product $(q'k)$, which includes the gluon momentum *k* and the photon momentum $\hat{q}$ in the trace [see Eq. (21)] in order to obtain the double logarithms.

Let us finally comment on a point which, at first sight, might look dangerous. Namely, starting from the spin structure

$$-\frac{M}{(pk)}i\varepsilon^{\mu\nu\alpha\beta}k_\alpha p_\beta\frac{(sk)}{(pk)} \tag{31}$$

in the lower nonsinglet part of Fig. 2, where the gluon momentum k_α plays the role of the photon momentum *q* in Eq. (1), it looks as if one might get a much larger small-*x* behavior, $g_2\sim 1/x$, than obtained in the previous discussions. In comparison with Eq. (14) this term $2(s^\perp k)\cdot i\varepsilon^{\mu\nu\alpha\beta}k_\alpha p_\beta \simeq k_t^2\cdot i\varepsilon^{\mu\nu\alpha\beta}s_\alpha\cdot p_\beta$ is enhanced by the factor $1/\beta_k$ as the longitudinal component of gluon momentum $k_\alpha\simeq\beta_k p'_\alpha$. However an extra factor $1/\beta_k$ destroys the logarithmic structure of

the $d\beta_k/\beta_k$ integral. Even more, we will show that such a contribution vanishes. Indeed, the integration in Fig. 2 over the rapidity of the upper horizontal quark line of the lower block $d\beta_{k'}/\beta_{k'}$ may be written in terms of the $x' = k^2/2(pk) \simeq k_t^2/2(pk)$ variable. This last quark with momentum $(k'-k)$ is on mass shell. So, keeping the transverse momenta k_t' and k_t fixed, we have

$$\beta_{k'} = \frac{|k'-k|_t^2}{\alpha_k S} = \frac{|k'-k|_t^2}{2p'k}$$

and therefore $d\beta_{k'}/\beta_{k'} = dx'/x'$.

On the other hand, we invoke the argument which leads to the Burkhardt-Cottingham sum rule [24]

$$\int_0^1 dx' g_2(x', Q^2) = 0. \tag{32}$$

This sum rule can be derived from an unsubtracted disperison relation for the photon-proton forward scattering amplitude. For the very special helicity structure which contributes to g_2, this amplitude leads to a cross section which falls with energy faster than $1/s$; therefore, the integral $\int ds' g_2(s')$ is finite, and from the large-s behavior of the dispersion relation one finds Eq. (32). The same large-$1/x$ condition applies to our starting function $g_2^{n.s.}$ (shown in [4]), therefore we conclude that

$$\int \frac{dx'}{x'} g_2(x', k^2) \frac{k_t^2}{(pk)} = \int dx' g(x', k^2) = 0. \tag{33}$$

Thus the term which looked so dangerous, in fact, does not contribute to double logarithmic structure function g_2.

V. INFRARED EVOLUTION EQUATIONS

With results of the previous sections we now turn to the infrared evolution equations (IREE). We are interested in the scattering of a virtual photon on a transversely polarized quark target: $T^s = T_1 + T_2$, and we will concentrate on the odd signature part. In order to formulate our coupled evolution equations, we first have to generalize to different target structures. As outlined in Sec. II, inside our diagrams we have to consider two different spin structures in the quark t-channel state (6),(7), labeled as q_s and q_k, and the gluon spin structure (10). Correspondingly we introduce the three component vector:

$$T = \begin{pmatrix} T(\gamma g) \\ T(\gamma q_k) \\ T(\gamma q_s) \end{pmatrix}. \tag{34}$$

For our scattering of a virtual photon on transversely polarized quark target we will be interested in the q_k component. We write T as a Mellin transform:

$$T = \int_{-i\infty}^{i\infty} \frac{d\omega}{2\pi i} \left(\frac{S}{\mu^2}\right)^{\omega} \xi(\omega) R(\omega, y), \tag{35}$$

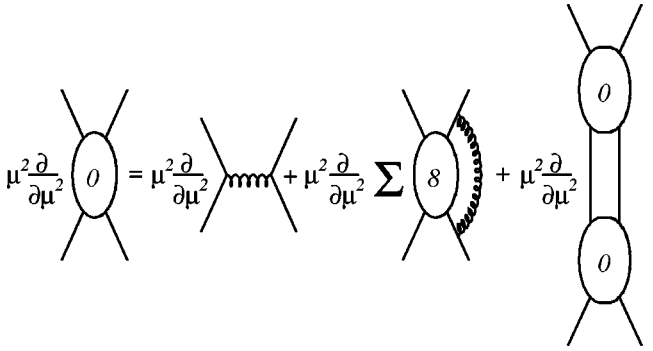

FIG. 3. Structure of the infrared evolution equations (IREE).

where $R(\omega, y)$ is a three-component vector, defined in analogy with Eq. (34), and $\omega = j$ denotes angular momentum. The signature factor $\xi(\omega) =$ has the form

$$= \frac{e^{-i\pi\omega} - 1}{2} \approx \frac{-i\pi\omega}{2}, \tag{36}$$

and

$$y = \ln\left(\frac{Q^2}{\mu^2}\right). \tag{37}$$

The structure function $g_\perp^s$ is obtained from the discontinuity (2), and we have to take into account both DL contributions and $i\pi$ terms. Before we can write down the IREE, we have to introduce further auxiliary quantities: scattering amplitudes F_{ij} (with $i,j = g, q_k, q_s$) which describe the scattering of quark or gluon with spin structure i on a target with structure j (loosely speaking, these scattering amplitudes are obtained if, in Fig. 2, we remove the coupling to the photon at the upper end). We write them as Mellin transforms, i.e. the F_{ij} are partial waves and depend upon angular momentum ω. By F_0 we denote the 3×3 matrix composed of the F_{ij} (the subscript refers to the color singlet quantum number):

$$F_0 = \begin{pmatrix} F_{gg} & F_{kg} & F_{sg} \\ F_{gk} & F_{kk} & F_{sk} \\ F_{gs} & F_{ks} & F_{ss} \end{pmatrix} \tag{38}$$

(it is the exact analogue to F_0 in [3] and to $f_0^{(-)}$ in [2]).

We now turn to the evolution equations. The IREE (illustrated in Fig. 3) describes the variation of the amplitude with respect to the infrared cutoff μ^2:

$$-\mu^2 \frac{\partial R}{\partial \mu^2} = \left(\omega + \frac{\partial}{\partial y}\right) R \quad . \tag{39}$$

This differential operator stands on the the left-hand side of the IREE for T, which is illustrated in Fig. 3. The right-hand side of the IREE is derived from the observation that the dependence upon the cutoff μ resides in the intermediate state with lowest virtuality (Fig. 3): the μ derivatives of the amplitudes are equal to R times quark or gluon scattering amplitudes F_{ij} with the external legs having transverse mo-

menta close to μ. In terms of the matrix F_0, the evolution equation for the vector R becomes

$$\left(\omega+\frac{\partial}{\partial y}\right)R=\frac{1}{8\pi^2}F_0R. \tag{40}$$

The matrix F_0 satisfies a nonlinear evolution equation (Fig. 3):

$$F_0(\omega)=\frac{g^2}{\omega}M_0-\frac{g^2}{2\pi^2\omega^2}G_0F_8(\omega)+\frac{1}{8\pi^2\omega}F_0(\omega)^2. \tag{41}$$

Here the matrix M_0 contains the evolution kernels (13) which we have computed in the previous section or collected from earlier studies:

$$M_0=\begin{pmatrix} 4C_A & -2T_F & 0 \\ 2C_F & C_F & 0 \\ 0 & -C_F & C_F \end{pmatrix}. \tag{42}$$

As we have discussed before, for the gluon state (upper left corner) the infrared evolution is described by the same splitting function as the singlet structure function g_1^s. For the two quark system in the lower right two by two block matrix we can use the results of [4]. The remaining matrix elements describe transitions from quark to gluon states, they are taken from the previous section. The second term on the RHS of Eq. (41) belongs to the gluon bremsstrahlung diagrams. The matrix G_0 has the form

$$G_0=\begin{pmatrix} C_A & 0 & 0 \\ 0 & C_F & 0 \\ 0 & 0 & C_F \end{pmatrix}. \tag{43}$$

In analogy to the matrix F_0 which carries color zero in the t channel we define the matrix F_8 of color octet amplitudes. Due to the antisymmetric color structure the elements of F_8 are even signature amplitudes. They satisfy evolution equations [19] similar to Eq. (41):

$$F_8=\frac{g^2}{\omega}M_8+\frac{g^2C_A}{8\pi^2\omega}\frac{d}{d\omega}F_8(\omega)+\frac{1}{8\pi^2\omega}F_8(\omega)^2. \tag{44}$$

The color factor C_A in front of the second term on the RHS is the analogue of the matrix G_0 in Eq. (41). The difference between C_A in Eq. (44) and G_0 in Eq. (41) is due to the fact that for the positive signature amplitude F_8 the sum of the two bremsstrahlung diagrams is independent of the type of the incoming partons, and the matrix of color factors G_8 becomes C_A times the unit matrix. Finally, the matrix M_8 is the analogue of the matrix M_0 in Eq. (41), but for color octet quantum numbers in the t channel instead of color singlet. It reads

$$M_8=\begin{pmatrix} 2C_A & -T_F & 0 \\ C_A & -1/2N_c & 0 \\ 0 & 1/2N_c & -1/2N_C \end{pmatrix}. \tag{45}$$

VI. SOLUTION OF THE EVOLUTION EQUATION

The solution for $g_\perp^s$, that is our vector T [Eq. (34) and (35)], is obtained by solving Eqs. (44) for F_8, then Eq. (41) for F_0 and Eq. (40) for R (the latter makes use of the Born approximation, R_B, as an initial condition for R), and finally inserting R into Eq. (35). The final answer for the three component vector T will have the form

$$T=\int\frac{d\omega}{2\pi i}\left(\frac{1}{x}\right)^\omega\xi(\omega)\left(\frac{Q^2}{\mu^2}\right)^{F_0/8\pi^2}\frac{1}{\omega-F_0/8\pi^2}R_B, \tag{46}$$

where

$$R_B=\begin{pmatrix} 0 \\ 2e_q^2 \\ 2e_q^2 \end{pmatrix}. \tag{47}$$

Let us go through these steps in somewhat more detail.

We begin with the equation for F_8. We first diagonalize the Born term, i.e. the matrix M_8. Thanks to the vanishing of the off-diagonal elements $(M_8)_{sg}=(M_8)_{sk}=0$ the two (largest) eigenvalues $\lambda^\pm$ coincide with the analogue eigenvalues for the DL evolution of the singlet function g_1^s. They are given by

$$\lambda_8^{(\pm)}=\frac{2C_A-1/2N}{2}\pm\frac{1}{2}\sqrt{(2C_A+1/2N)^2-4C_AT_F} \tag{48}$$

and

$$\lambda_8^{(s)}=-\frac{1}{2N_c}. \tag{49}$$

Let $e^{(+)}$,$e^{(-)}$ and $e^{(s)}$ denote the eigenvectors of M_8:

$$e^{(+)}=\begin{pmatrix} 1 \\ x^{(+)} \\ y^{(+)} \end{pmatrix},\quad x^{(+)}=\frac{\lambda^{(+)}-M_{11}}{M_{12}},$$

$$y^{(+)}=\frac{\lambda^{(s)}x^{(+)}}{\lambda^{(s)}-\lambda^{(+)}} \tag{50}$$

and

$$e^{(-)}=\begin{pmatrix} x^{(-)} \\ 1 \\ y^{(-)} \end{pmatrix},\quad x^{(-)}=\frac{\lambda^{(-)}-M_{22}}{M_{21}},$$

$$y^{(-)}=\frac{\lambda^{(s)}}{\lambda^{(s)}-\lambda^{(-)}}. \tag{51}$$

The last eigenvector corresponds to the pure quark eigenvalue $\lambda=\lambda_8^{(s)}$ and reads

$$e^{(s)}=\begin{pmatrix}0\\0\\1\end{pmatrix}. \tag{52}$$

Denote by $E_8=(e^{(+)},e^{(-)},e^{(s)})$ the matrix composed of these eigenvectors. For the diagonalization we also need its inverse E_8^{-1}:

$$E^{-1}=\frac{1}{1-x^{(+)}x^{(-)}}\begin{pmatrix}1 & -x^{(-)} & 0\\ -x^{(+)} & 1 & 0\\ b^{(+)} & b^{(-)} & 1-x^{(+)}x^{(-)}\end{pmatrix}, \tag{53}$$

where

$$b^{(+)}=y^{(-)}x^{(+)}-y^{(+)},\qquad b^{(-)}=y^{(+)}x^{(-)}-y^{(-)}. \tag{54}$$

Then we can diagonalize the matrix M_8

$$M_8=E_8\hat{M}_8E_8^{-1}, \tag{55}$$

where $\hat{M}_8=\mathrm{diag}(\lambda_8^+,\lambda_8^-,\lambda_8^{(s)})$. Consequently, Eq. (44) becomes diagonal if we transform to $\hat{F}_8$:

$$F_8=E_8\hat{F}_8E_8^{-1}. \tag{56}$$

Using the ansatz $\hat{F}_8^i=N_cg^2(\partial/\partial\omega)\ln u^i(\omega)$ for the nonlinear Riccati equation (43), one finds second order linear differential equations for the u^i. Their solutions are given by parabolic cylinder functions. As a result we find for the components of $\hat{F}_8$

$$\hat{F}_8^i=N_cg^2\frac{\partial}{\partial\omega}\ln e^{z^2/4}D_{p_i}(z), \tag{57}$$

where D_p denotes the parabolic cylinder function with

$$p_i=\frac{\lambda_8^{(i)}}{N_c}\qquad(i=+,-,s) \tag{58}$$

and

$$z=\frac{\omega}{\omega_0},\qquad \omega_0=\sqrt{N_cg^2/8\pi^2}. \tag{59}$$

With this solution for F_8 we return to the evolution equation (41) for F_0 which is solved by the (matrix-valued) expression:

$$\frac{1}{4\pi^2\omega}F_0=1-\sqrt{1-\frac{g^2}{2(\pi\omega)^2}M_0+\frac{g^2}{4\pi(\pi\omega)^3}G_0F_8}. \tag{60}$$

We will need the right-most singularity in the ω plane of the matrix F_0. Similar to the case of g_1, this singularity is due to the vanishing of the square root in Eq. (60), i.e. we need to determine the zeros of the eigenvalues of the matrix under the square root. The diagonalization of this matrix is done in exactly the same way as for M_8: again, the matrix elements "sg" and "sk" are zero, and the two largest eigenvalues are the same as for the singlet function g_1. The diagonalization is done through the matrix E_0 which consists of the corresponding three eigenvectors $e_0^{(+)}$, $e_0^{(-)}$ and $e_0^{(s)}$ [analogous to Eqs. (50)–(52)]. As was discussed in [3], the largest eigenvalue $\lambda^{(+)}$ is not too far from the value obtained in the pure gluonic case, neglecting the quark contribution. The accurate values have to be found from a numerical computation of the parabolic cylinder functions. For the case of $n_F=4$ we found in [3] the rightmost singularity $\omega_s=3.45\omega_0$ (the pure gluonic case would have given 3.66 instead of 3.45, or even 4 if one neglects the nonladder DL contribution). With ω_0 from Eq. (59) and $\alpha_s=0.18$ we find for the leading term in Eq. (46)

$$\omega_s=1.01. \tag{61}$$

Two other singularities correspond (for $n_F=4$) to $z^{(-)}=1.81$ and $z^s=1.39$.

Having found the matrix F_0, we return to Eq. (40) and find the matrix R:

$$R=\left(\frac{Q^2}{\mu^2}\right)^{F_0/8\pi^2-\omega}\hat{R}(\omega) \tag{62}$$

where the matrix valued function $\hat{R}(\omega)$ has to be determined from the initial conditions of the evolution equation from the energy dependence of R at the point $y=0$, i.e. at $Q^2=\mu^2$. At this point the matrix R satisfies another evolution equation which has been discussed in detail in [2,21] [after Eq. (3.14)], and its solution has the form

$$\hat{R}(\omega)=E_0\frac{1}{\omega-\hat{F}_0/8\pi^2}E_0^{-1}R_B. \tag{63}$$

Retaining in $\hat{F}_0$ only the leading upper component we find for the behavior of R near the square root branch point at $\omega=\omega_s$

$$R(\omega,y)\sim\frac{-2e_q^2\cdot x^{(-)}}{1-x^{(+)}x^{(-)}}\begin{pmatrix}1\\x^{(+)}\\y^{(+)}\end{pmatrix}\frac{2}{\omega_s}\left(\frac{Q^2}{\mu^2}\right)^{\omega_s/2} \tag{64}$$

with $x^{(+)}=0.29$, $x^{(-)}=0.43$, $y^{(+)}=-0.052$, and $y^{(-)}=-1.40$. Without the nonladder contribution [i.e. putting ($F_8=0$)] we would have $x^{(+)}=0.28$ and $y^{(+)}=-0.039$.

Finally, to obtain the structure function g_2^s we have to subtract the known function g_1^s [3] ($g_2=g_\perp-g_1$), and add the positive signature part ($-g^L/2$) given by the same pure ladder DL evolution as in the nonsinglet case [4]:

$$g_\perp=g_1+g_2 = \int \frac{d\omega}{2\pi i}\left(\frac{1}{x}\right)^\omega \xi(\omega)\left(\frac{Q^2}{\mu^2}\right)^{\hat{F}_0/8\pi^2} \times E_0 \frac{1}{\omega-\hat{F}_0/8\pi^2} E_0^{-1} R_B - g^L/2. \quad (65)$$

VII. CONCLUSIONS

In this paper we have studied the small-x behavior of the singlet polarized structure function g_2, using the double logarithmic approximation. Our analysis is based upon ladder-type Feynman diagrams, but in order to make our DLA study complete, we had to take into account also the bremsstrahlung of soft gluons. We have shown that, at small x, the leading contribution to $g_2^s(x,Q^2)$ is given by the convolution of the nonsinglet spin dependent distribution [corresponding to the quark density matrix $(s^\perp k)\gamma_5\hat{k}$] with the singlet function g_1^s. As a novel feature, g_2 contains pieces with different signature, both for the nonsinglet and for the singlet case. At small x, we therefore have to decompose the Feyman diagrams, in order to separate even and odd signature. The small-x asymptotic behavior of the structure function g_2^s comes from the odd-signature part of the amplitude and is driven by the asymptotics of the singlet spin dependent function g_1^s. At $1/x\to\infty$ we have found

$$g_2 \propto \left(\frac{1}{x}\right)^{\omega_s}\left(\frac{Q^2}{\mu^2}\right)^\gamma, \quad (66)$$

where the anomalous dimension γ has the value

$$\gamma=\omega_s/2 \quad (67)$$

and

$$\omega_s \simeq 3.45\sqrt{\alpha_s N_c/2\pi} \quad (68)$$

(the latter result holds for $n_F=4$). In contrast to the unpolarized case, at small x the gluons mix with the quarks. As in the singlet polarized structure function g_1^s, the dominant contribution comes from the t-channel two gluon states. This is mainly due to the color charge of the gluon which is much larger than that of the quark. Numerically the value of ω_s is rather large: $\omega_s\simeq 1.01$ for $\alpha_s=0.18$. This value of ω_s is considerably larger than the value of corresponding ''intercept'' of the nonsinglet function $g_2^{n.s.}$. It is also larger than the even signature part $-g^L/2$ of the singlet g_2^s, where $\omega_{n.s.}=\omega_0=\sqrt{(2C_F\alpha_s)/\pi}$ (the ratio of the two values ω_s/ω_0 is about 2.6). Therefore the asymptotic behavior of the spin dependent singlet structure function $g_2^s(x,Q^2)$ is almost completely driven by the DL behavior of the singlet $g_1^s(x,Q^2)$ distribution.

From the formal point of view, the double logarithmic approximation (DL) that we have been using here (i.e., the neglect of nonlogarithmic contributions) can be justified only for the case of a very small QCD coupling $\alpha_s\ll 1$, in which case also ω_s is small. The experience from the LO and NLO Balitskiĭ-Fadin-Kuraev-Lipatov (BFKL) calculations supports the belief that, whenever the leading approximation turns out to be large, one has to expect also large NLO corrections. Thus one should be careful in using the DL results for the singlet structure function for the numerical applications. Nevertheless, our findings indicate that the singlet spin dependent structure function g_2^s grows steeply at $x\to 0$.

ACKNOWLEDGMENTS

J.B. was supported by the EU TMR-Network ''QCD and the Deep Structure of Elementary Particles,'' contract number FMRX-CT98-0194 (DG 12-MIHT). The work of M.G.R. was supported by the NATO Collaborate Linkage Grant SA (PST.CLG.976453)5437 and by the RFFI grant 00-15-96610.

[1] G. Altarelli and G. Parisi, Nucl. Phys. **B126**, 297 (1977).
[2] J. Bartels, B.I. Ermolayev, and M.G. Ryskin, Z. Phys. C **70**, 273 (1996).
[3] J. Bartels, B.I. Ermolayev, and M.G. Ryskin, Z. Phys. C **72**, 627 (1996).
[4] J. Bartels and M.G. Ryskin, Phys. Rev. D **63**, 094002 (2001).
[5] A.J.G. Hey and J.E. Mandula, Phys. Rev. D **5**, 2610 (1972).
[6] S. Wandzura and F. Wilczek, Phys. Lett. **72B**, 195 (1977).
[7] J. Bluemlein and N. Kochelev, Phys. Lett. B **381**, 296 (1996); Nucl. Phys. **B498**, 285 (1997); J. Blumlein and A. Tkabladze, *ibid.* **B553**, 427 (1999).
[8] G. Altarelli, B. Lampe, P. Nason, and G. Ridolfi, Phys. Lett. B **334**, 187 (1994).
[9] A. Harindranath and Wei-Min Zhang, Phys. Lett. B **408**, 347 (1997).
[10] A. Gabrieli and G. Ridolfi, Phys. Lett. B **417**, 369 (1998).
[11] A.P. Bukhvostov, E.A. Kuraev, and L.N. Lipatov, Sov. Phys. JETP **60**, 22 (1984).
[12] J. Kodaira, Y. Yasui, and T. Vematsu, Phys. Lett. B **344**, 348 (1995).
[13] A. Ali, V.M. Braun, and G. Hiller, Phys. Lett. B **266**, 117 (1991).
[14] K. Sasaki, Phys. Rev. D **58**, 094007 (1998).
[15] V.M. Braun, G.P. Korchemsky, and A.N. Manashov, Phys. Lett. B **476**, 455 (2000).
[16] V.M. Braun, G.P. Korchemsky, and A.N. Manashov, Nucl.

Phys. **B597**, 370 (2001); **B603**, 69 (2001).
[17] B. L. Ioffe, V. A. Khoze, and L. N. Lipatov, *Hard Processes* (North-Holland, Amsterdam, 1984).
[18] R.L. Heimann, Nucl. Phys. **B64**, 429 (1973).
[19] R. Kirschner and L.N. Lipatov, Nucl. Phys. **B213**, 122 (1983).
[20] V.N. Gribov, V.G. Gorshkov, G.V. Frolov, and L.N. Lipatov, Sov. J. Nucl. Phys. **6**, 95 (1967).
[21] B.I. Ermolayev, S.I. Manaenko, and M.G. Ryskin, Z. Phys. C **69**, 259 (1996).
[22] L. N. Lipatov (private communication).
[23] J. Bartels, L.N. Lipatov, and G.P. Vacca, Phys. Lett. B **477**, 178 (2000).
[24] H. Burkhardt and W.N. Cottingham, Ann. Phys. (N.Y.) **56**, 453 (1970).